THE JOURNAL OF BIOLOGICAL CHEMISTRY VOL. 286, NO. 49, pp. 42267–42273, December 9, 2011

Delayed Re-epithelialization in Ppm1a Gene-deficient Mice Is Mediated by Enhanced Activation of Smad2*[S]

Received for publication, August 10, 2011, and in revised form, October 5, 2011 Published, JBC Papers in Press, October 11, 2011, DOI 10.1074/jbc.M111.292284

Xue Yang[‡§1], Yan Teng[‡1,2], Ning Hou[‡], Xiongwei Fan[‡¶], Xuan Cheng[‡], Jun Li[‡], Lijuan Wang[‡], Youliang Wang[‡], Xiushan Wu[¶], and Xiao Yang[‡§3]

From the [‡]State Key Laboratory of Proteomics, Genetic Laboratory of Development and Disease, Institute of Biotechnology, Beijing 100071, P.R. China, the [§]Model Organism Division, E-institutes of Shanghai Universities, Shanghai JiaoTong University, Shanghai 200025, P.R. China, and the [¶]College of Life Sciences, Hunan Normal University, Changsha 410081, P.R. China

Background: The *in vivo* function of Ppm1a in mammals remains unknown.
Results: Mice lacking Ppm1a developed normally but showed delayed re-epithelialization with retarded keratinocyte migration caused by overactivation of Smad2 during cutaneous wound healing.
Conclusion: Ppm1a, through suppressing Smad2-mediated signaling, plays a critical role in re-epithelialization.
Significance: We provided the first direct and critical genetic evidence of the *in vivo* role of Ppm1a.

Protein phosphatase magnesium-dependent 1A (PPM1A), a protein serine/threonine phosphatase, controls several signal pathways through cleavage of phosphate from its substrates. However, the *in vivo* function of Ppm1a in mammals remains unknown. Here we reported that mice lacking Ppm1a developed normally but were impaired in re-epithelialization process during cutaneous wound healing. Specifically, complete or keratinocyte-specific deletion of Ppm1a led to delayed re-epithelialization with reduced keratinocyte migration upon wounding. We showed that this effect was the result of an increase in Smad2/3 phosphorylation in keratinocytes. Keratinocyte-specific Smad2 deficient mice displayed accelerated re-epithelialization with enhanced keratinocyte migration. Importantly, Smad2 and Ppm1a double mutant mice also exhibited accelerated re-epithelialization, demonstrating that the effect of Ppm1a on promoting re-epithelialization is mediated by Smad2 signaling. Furthermore, the decreased expression of specific integrins and matrix metalloproteinases (MMPs) may contribute to the retarded re-epithelialization in Ppm1a mutant mice. These data indicate that Ppm1a, through suppressing Smad2 signaling, plays a critical role in re-epithelialization during wound healing.

Cutaneous wound healing comprises three well-defined temporally overlapping stages: inflammation, new tissue formation with synthesis of new connective tissue and epithelial wound closure (re-epithelialization), and remodeling (1). Re-epithelialization, which is responsible for the rapid restoration of an intact epidermal barrier with neo-epidermis, necessitates keratinocyte migration, proliferation, and differentiation (2). Re-epithelialization is influenced by a combination of growth factors, including hepatocyte growth factor (HGF), fibroblast growth factors (FGFs), epidermal growth factor (EGF), heparin-binding epidermal growth factor (HB-EGF), as well as transforming growth factor-β (TGF-β) in a temporospatial manner (2).

TGF-β binds to its receptors at the cell surface, facilitating phosphorylation of the type I receptor (TβRI) by the type II receptor (TβRII). The activated TβRI then phophorylates the receptor-activated Smads (R-Smads), Smad2 and Smad3, at two serines in their C-terminal SXS motifs. The phosphorylated Smad2/3 complex associates with the common Smad (Co-Smad), Smad4, which translocates to the nucleus and regulates expression of specific target genes, leading to a particular biological response (3, 4). Studies from TGF-β1 or Smad4 knockout mice and activin A transgenic mice have indicated that TGF-β signaling pathway promotes re-epithelialization during cutaneous wound healing (5–7). However, overwhelming evidence from genetic alteration of other TGF-β/Smad signaling components, such as overexpression of TGF-β1, BMP6, Smad2, or dominant negative type II TGF-β receptor, and loss of Smad3, supports the inhibitory effects of TGF-β signaling on re-epithelialization (8–15). Recently, Dpr2, α3-integrin and β3-integrin have been shown to regulate the rate of re-epithelialization by modulating TGF-β signaling (16–18). Therefore, identifying new regulators of TGF-β/Smad pathway involved in re-epithelialization will be helpful for better understanding of the sophisticated roles of TGF-β signaling in wound healing.

Protein phosphatase magnesium-dependent 1A (PPM1A),[4] belonging to PPM family, is a metal-ion-dependent phosphatase that cleave phosphate from phosphorylated serine and threonine residues (19). A number of substrates of PPM1A have

* This work was supported by Grants 2011CB504200, 2012CB945100, and 2011CB910601 from the Chinese National Key Program on Basic Research, Grants 31030040, 30871396, 31171249, and 30700423 from the National Natural Science Foundation of China, and Grant 5082018 from the Beijing Natural Science Foundation of China.
[S] The on-line version of this article (available at http://www.jbc.org) contains supplemental Figs. S1–S4.
[1] Both authors contributed equally to this work.
[2] To whom correspondence may be addressed: Institute of Biotechnology, 20 Dongdajie, Beijing 100071, P.R. China. E-mail: tengyan0919@tom.com.
[3] To whom correspondence may be addressed: Institute of Biotechnology, 20 Dongdajie, Beijing 100071, P.R. China. Tel./Fax: 86-10-63895937(O); E-mail: yangx@nic.bmi.ac.cn.

[4] The abbreviations used are: PPM1A, protein phosphatase magnesium-dependent 1A; MMP, matrix metalloproteinase; PI3K, phosphatidylinositol 3-kinase; ES, embryonic stem.

been identified, including p38 kinase (20), phosphatidylinositol 3-kinase (PI3K) (21), Cdk2 (22), Axin (23), and Smads (19, 24). As the first identified phosphatase capable of catalyzing dephosphorylation of Smad2/3, PPM1A decreases the cellular responses to TGF-β (19, 25). PPM1A has also been shown to suppress BMP signaling dependent or independent of Smad dephosphorylation (24, 26). However, the *in vivo* function of PPM1A in mammals and its functional substrates remain unknown.

In the present study, we generated complete Ppm1a gene knock-out mice and found that Ppm1a was dispensable for normal embryonic and postnatal development. We, therefore, analyzed the wound healing phenotypes of two *in vivo* models of Ppm1a deficiency and demonstrated that Ppm1a promoted re-epithelialization by suppressing Smad2-mediated signaling.

EXPERIMENTAL PROCEDURES

Generation of Ppm1a Mutant Mice—A 13 kb genomic fragment, comprising the 4 kb 5′-region, the LoxP-floxed exon 2 and exon 3, and the 3 kb 3′-region, were cloned into the Pfrt1 vector containing a FRT-floxed neomycin resistance cassette and a TK cassette. The neomycin cassette was inserted 300 bp upstream of exon 2, and the other LoxP was inserted 3.5 kb downstream of exon 3. NotI-linearized targeting vector was electroporated into TC1 mouse embryonic stem (ES) cells (27). Correct targeted ES cells were confirmed by Southern blot analysis. The chimeric mice were generated by microinjection of targeted ES cells into C57BL/6J blastocysts.

Genotyping by PCR Analysis—Ppm1a primer 1 (5′-AGCACCTGGTCAGCATCTTG-3′) and primer 2 (5′-ACTTTGACTACACGAGCTTGAGA-3′) from Ppm1a genomic sequence amplified a 221 bp or a 320 bp fragment from the wild-type allele or the conditional knock-out allele. The combinatory use of primer 2 and primer 3 from neomycin cassette (5′-TGGGGATGCGGTGGGCTCTAT-3′) amplified a 450 bp fragment from the complete mutant allele. Smad2 primer 4 (5′-TGCCCACACAAACCTTTCCTG-3′) and primer 5 (5′-TTGGGGGAAGACAAGTGGATT-3′) from Smad2 genomic sequence amplified a 251 bp or a 301 bp fragment from the wild-type or the conditional knock-out allele. The Cre gene was identified by primer 6 (5′-TGGTTGTCAATACTCCTGGTCCTG-3′) and primer 7 (5′-TTGCGAACCTCATCACTCGTTG-3′).

RNA Isolation and Real-time PCR—Total RNA was extracted from mice using TRIzol reagent (Invitrogen), and used for reverse transcription with mRNA Selective PCR kit (Takara). Real-time PCR was performed by a SYBR Green assay with Roche Light Cycler 1.5 system. Expression values were normalized to GAPDH expression. The primer sequences were as follows: integrin αv: 5′-CCCAAAGCGAACACGACC-3′ and 5′-CACAGAGGCTCCAAACCA-3′; integrin β1: 5′-GGGGTATTTGTGAATGTGGTGC-3′ and 5′-CTTTGGTGAGATTGAAGTGGGAG-3′; integrin α5: 5′-CACATTGCCCTCAACTTCT-3′ and 5′-CTTGTCCTCTATCCTGCTTTT-3′; MMP2: 5′-CAAGAGCGTGAAGTTTGG-3′ and 5′-TACAGAGGAGGACAGAGCC-3′; MMP13: 5′-CCCTTGATGCCATTACCA-3′ and 5′-GTCACGGGATGGATGTTC-3′; GAPDH: 5′-TGCCCAGAACATCATCC CT-3′ and 5′-GGTCCTCAGTGTAGCCCAAG-3′.

In Vivo Wound-healing Experiments—Littermates at 6–8 weeks of the same sex were used. Four 4-mm full-thickness cutaneous biopsy punch wounds were generated in the back skin of the gene-deficient mice and control littermates (16). The mice were killed at different time points (3, 5, 7 days) after injury and wounds were excised including 2 mm of the epidermal margins for RNA or protein isolation. Wounded tissue was removed and fixed overnight in cold 4% PFA for paraffin or snapfrozen in OCT (Thermo Lifesciences). The wound width was quantitated by measuring the distance between epithelial edges across the wound bed. The width of wound sites minus the wound width was neo-epithelial length.

Histological Analysis, Immunohistochemistry, and Immunofluorescence—Mouse tissues were embedded in paraffin, sectioned at 6 μm, and stained with hematoxylin and eosin (H&E) or analyzed by immunological methods. For BrdU labeling, mice were injected intraperitoneally with 100 μg/g body weight of BrdU (Sigma) 2 h before sacrifice. For immunohistochemistry and immunofluorescence, the slides were incubated with K14 antibody (1:1000, Covance) and BrdU antibody (1:300, Abcam), followed by incubation with FITC-conjugated anti-rabbit IgG and TRITC-conjugated anti-rat IgG, or biotin-conjugated goat anti-rabbit IgG (all 1:100, Zhongshan, Beijing). Signals were detected by DAB (Zhongshan, Beijing) staining or directly by fluorescence microscopy. Slides were observed under a Nikon E600 microscope (Tokyo, Japan) with a digital camera.

Preparation and in Vitro Culture of Keratinocytes—Primary mouse keratinocytes were isolated from skin of newborn mice. Full thickness skin was treated with 5 mg/ml Dispase (Invitrogen) solution overnight (14∼16 h) at 4 °C. The epidermis was gently separated from the dermis and transferred onto the surface of the drop of TrypLE Select (Invitrogen) with the basal layer downward. The epidermis was incubated for 20–30 min at room temperature, followed by suspending in Keratinocyte-SFM medium with supplements (Invitrogen). Cells were separated from the epidermis and incubated in dishes coated with coating solution (10 μg/ml fibronectin, 1% v/v vitrogen 100 collagen, 100 μg/ml BSA, 10 mM HEPES) at 34 °C in 5% CO_2. Attached cells were further cultured in fresh Keratinocyte-SFM medium with supplements and 5% fetal bovine serum (Hyclone), which was replaced once every 2 days.

Western Blot—The protein from the wounded edge of mice was collected at days 0, 3, and 5 after injury. The tissue lysates were separated by 12% SDS-polyacrylamide gels and transferred onto polyvinylidene fluoride membranes (Bio-Rad). Antibodies used included Ppm1a, Smad2, p-Smad2/3, total Smad2/3, p-Smad2, total Smad2, p-Smad3, total Smad3 (1:1000, CST), and GAPDH (1:2000, Zhongshan, Beijing) was used as a loading control.

In Vitro Scratch Closure Assay—The 80–90% confluent keratinocytes in 6-well plates were treated with 10 μg/ml mitomycin C (Sigma) for 2 h to remove the influence of cell proliferation. Cells were then scratched with a pipette tip. Cell migration was monitored by microscopy at 0 and 48 h after wounding. The images acquired for each sample can be further analyzed

quantitatively. For each image, distances between one side of scratch and the other can be measured. By comparing the images from time 0 to 48 h, we obtain the distance of each scratch closure on the basis of the distances that are measured by software.

Statistical Analysis—All values were expressed as mean ± S.D. Statistical analysis of the data were performed by two-tailed Student's *t* test. *, $p < 0.05$; **, $p < 0.01$.

RESULTS

Normal Embryonic Development in Complete Ppm1a-deficient Mice—The Cre-LoxP site-specific recombination system was used to target Ppm1a for complete and conditional deletion in mouse. To generate the Ppm1a targeting construct, a neomycin (neo) resistance cassette flanked by two FRT sites and a single LoxP site is inserted into the upstream of exon 2 of Ppm1a gene, and the second LoxP site was introduced into intron 3 (supplemental Fig. S1*A*). This targeting construct was electroporated into mouse ES cells. The homologous recombinant ES clones were determined by Southern blotting analysis (data not shown), and were injected into blastocysts to generate chimeric mice. The chimeric mice exhibited germline transmission of the LoxP-floxed Ppm1a allele ($Ppm1a^{fl/+}$). $Ppm1a^{fl/+}$ mice were bred with EIIa-Cre mice (28) to generate complete Ppm1a-deficient mice ($Ppm1a^{-/-}$) (supplemental Fig. S1*B*).

Murine Ppm1a was expressed in a ubiquitous manner, including in various adult tissues and embryos (supplemental Fig. S1*C*). To evaluate the efficiency of Ppm1a excision in $Ppm1a^{-/-}$ mice, we detected the RNA from a number of tissues by RT-PCR analysis, and verified that no detectable Ppm1a transcripts were found in liver, stomach, and skin tissues from $Ppm1a^{-/-}$ mice (supplemental Fig. S1*D*).

$Ppm1a^{-/-}$ mice were born with Mendelian frequencies, and presented no genotype dependent differences in gross morphological abnormalities, or fertility. These findings indicated that Ppm1a was not essential for normal embryonic development.

Deletion of Ppm1a Led to Delayed Re-epithelialization during Wound Healing via Decreased Keratinocyte Migration—To investigate the role of Ppm1a during cutaneous wound healing, full-thickness 4-mm punch biopsies were made in the back skin of wild-type mice. Interestingly, we found that, after injury, the amount of Ppm1a at wound edge was decreased by 25 and 80% at days 1 and 3, respectively (Fig. 1*A*). This raises a question of whether or not Ppm1a is required for normal wound healing. Thus, we explored the consequence of Ppm1a deletion during wound healing. As expected, Ppm1a protein was detectable in whole skin tissue or in the isolated primary keratinocytes from control heterozygous mice ($Ppma^{+/-}$), but was undetectable from $Ppm1a^{-/-}$ mice (Fig. 1*B*). The healing process was analyzed at days 3, 5, and 7 days after injury ($n = 5$ for each time point and genotype). Wounds were immunostained with Keratin 14 antibody for examination of re-epithelialization (measured by wound widths and lengths of neo-epithelium). Because the re-epithelialization rate in heterozygous mice ($Ppm1a^{+/-}$) was comparable with that in wild-type mice (data not shown), we used the $Ppm1a^{+/-}$ mice as controls in this study. We observed that the re-epithelialization in $Ppm1a^{-/-}$ mice was

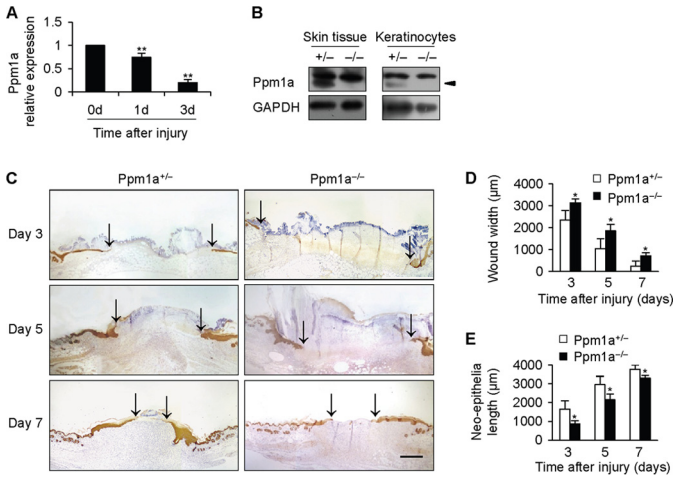

FIGURE 1. **Deletion of Ppm1a led to delayed re-epithelialization during wound healing.** *A*, Ppm1a expression was detected by real-time PCR at wound edge at days 0, 1 and 3 after injury. *B*, Western blot analysis revealed loss of Ppm1a protein in skin tissue and primary keratinocytes from $Ppm1a^{-/-}$ mice. *Arrows* indicated the specific band of Ppm1a. *C*, sections of wounded skin of $Ppm1a^{-/-}$ and control mice were immunostained with K14 antibody (*brown*) at days 3, 5, and 7 after injury. *Arrows* indicated the leading edges of wounded epidermis. *D* and *E*, quantitative analyses of wound width (*D*) and neo-epithelia length (*E*). $n = 5$. Values represent mean ± S.D. *, $p < 0.05$; **, $p < 0.01$. Scale bar: 400 μm (*C*).

markedly delayed compared with that of control littermates (Fig. 1*C*). The wound widths were larger and neo-epithelial lengths were shorter at days 3, 5, 7 in $Ppm1a^{-/-}$ healing skin than controls (Fig. 1, *D* and *E*; $p < 0.05$). In addition, the granulation tissue formation in both Ppm1a-null and control mice occurred comparably at day 5 (data not shown).

Re-epithelialization is mainly dependent on keratinocyte migration and keratinocyte proliferation (2). There was a comparable number of cells proliferating at wound edge from $Ppm1a^{-/-}$ and control mice, as determined by bromodeoxyuridine (BrdU) labeling (Fig. 2, *A* and *B*). To assess whether loss of Ppm1a affected keratinocyte migration, primary keratinocytes were isolated from $Ppm1a^{-/-}$ and control newborn mice, and an *in vitro* scratch assay, in which a "wound" is introduced in cultured monolayer keratinocytes, was performed. The rate of scratch closure from $Ppm1a^{-/-}$ keratinocytes was notably slower by 37% than that from controls at 48 h after wounding (Fig. 2, *C* and *D*; $p < 0.01$), suggesting that delayed re-epithelialization observed in Ppm1a mutant mice might be attributable to reduced keratinocyte migration.

To clarify whether or not Ppm1a-deficient keratinocytes, but not other cell types, mainly accounted for the delayed re-epithelialization observed in $Ppm1a^{-/-}$ mice, we generated keratinocyte-specific Ppm1a mutant ($K5\text{-}Cre;Ppm1a^{fl/fl}$) mice by breeding $Ppm1a^{fl/fl}$ mice with *K5-Cre* transgenic mice (29, 30). Dramatic reduction of Ppm1a was demonstrated in the isolated Ppm1a mutant primary keratinocytes (supplemental Fig. S2*A*). Similar to complete Ppm1a-null mice, $K5\text{-}Cre;Ppm1a^{fl/fl}$ mice also exhibited impaired re-epithelialization and retarded keratinocyte migration (supplemental Fig. S2, *B–F*), suggesting that Ppm1a in keratinocytes was responsible for maintaining the normal rate of re-epithelialization during wound healing.

Overactivation of Smad2 in Ppm1a-deficient Mice—Previous studies have shown that Ppm1a could modulate Smad and

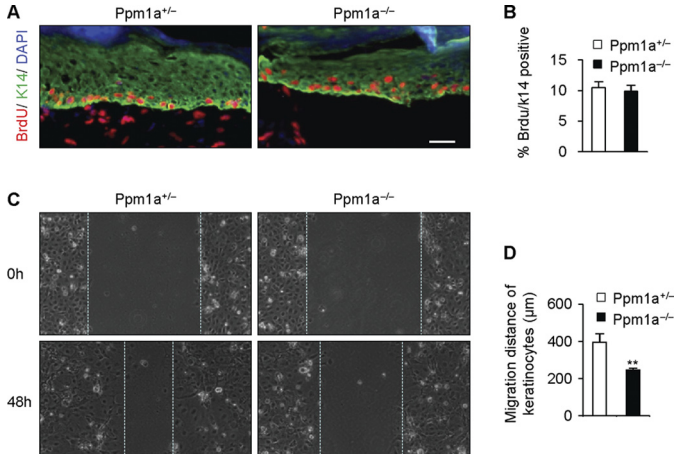

FIGURE 2. **The reduced keratinocyte migration contributed to the delayed re-epithelialization in the Ppm1a-deficient mice.** *A*, immunofluorescence staining with BrdU (*red*) and K14 (*green*) antibodies was carried out at day 3 after injury in *Ppm1a*$^{-/-}$ and control wound sections. No obvious difference was found in percentage of BrdU positive keratinocytes in *Ppm1a*$^{-/-}$ and control mice. *B*, quantification of the percentage of BrdU-positive keratinocytes; $n = 3$. *C*, scratch wound-healing assay was conducted in the *Ppm1a*$^{-/-}$ and control keratinocyte monolayers. Migration distance was measured at 0, 48 h after cells were scratched. *D*, quantification of migration distance. $n = 3$. Values represent mean ± S.D. *, $p < 0.05$; **, $p < 0.01$. Scale bar: 50 μm (*A*)

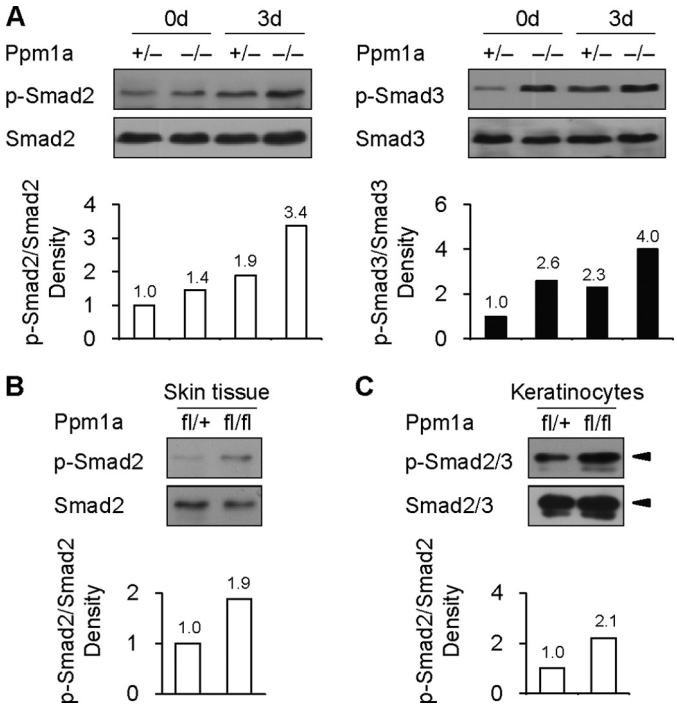

FIGURE 3. **Ppm1a-deficient mice displayed overactivation of Smad2 post-wounding.** *A*, Western blot was performed to detect expression of phosphorylated Smad2 (p-Smad2) and Smad3 (p-Smad3) and total Smad2 and Smad3 at wound edge of *Ppm1a*$^{-/-}$ and control mice at days 0 and 3 after injury. Each protein sample was a mixture of 3 mice with the same genotype. *Bar charts* represent densitometry results. *B*, Western blot analysis showed that p-Smad2 was increased at the wound edge of *K5-Cre;Ppm1a*$^{fl/fl}$ mice. Each protein sample was a mixture of 3 mice with the same genotype. Bar charts represent densitometry results. *C*, Western blot revealed the up-regulation of p-Smad2/3 expression in the primary keratinocytes from *K5-Cre;Ppm1a*$^{fl/fl}$ mice. *Arrows* indicated the specific band of p-Smad2 and Smad2. *Bar charts* represent densitometry results.

PI3K/Akt signaling pathways, both of which are involved in wound healing process and keratinocyte migration (9, 12, 19, 21, 31). So we checked the expression levels of p-Akt and p-Smad2/3 at wound edge from Ppm1a-null and control mice by Western blot. p-Akt expression remained unchanged in Ppm1a-null mice compared with control mice post-wounding (supplemental Fig. S3*A*). Both p-Smad2 and p-Smad3 were up-regulated in control mice 3 days after injury, and were profoundly increased in Ppm1a-null mice compared with that in controls before and after wounding (Fig. 3*A*). The up-regulation of p-Smad2 was also detected at wound edge of keratinocyte-specific Ppm1a mutant (*K5-Cre;Ppm1a*$^{fl/fl}$) mice (Fig. 3*B*). Consistently, the increased expression of p-Smad2/3 was observed in the isolated primary keratinocytes of *K5-Cre;Ppm1a*$^{fl/fl}$ mice (Fig. 3*C*). In addition, Smad2 expression was not changed after Ppm1a deletion (supplemental Fig. S3*B*). These data suggested that enhanced activation of Smad2/3 signaling in keratinocytes possibly contributed to the delayed re-epithelialization in Ppm1a-null mice.

Keratinocyte-specific Smad2 Deletion Resulted in Accelerated Re-epithelialization—To determine if keratinocytic Smad2 plays a critical role during wound healing, we generated keratinocyte-specific Smad2 mutant (*K5-Cre;Smad2*$^{fl/fl}$) mice by breeding *Smad2*$^{fl/fl}$ mice (32) with *K5-Cre* transgenic mice. Although mice with keratinocyte-specific Smad2 deletion exhibit accelerated formation and malignant progression of chemically induced skin tumors (33), the consequence of keratinocyte-specific Smad2 deletion in wound healing remains unknown. Western blot confirmed that Smad2 expression was significantly down-regulated in primary keratinocytes of *K5-Cre;Smad2*$^{fl/fl}$ mice (Fig. 4*A*). In contrast to Ppm1a-null mice, the rate of re-epithelialization was markedly accelerated in *K5-Cre;Smad2*$^{fl/fl}$ mice compared with controls (Fig. 4, *B–D*). The wound widths were smaller and neo-epithelial lengths were longer at days 3, 5, 7 in *K5-Cre;Smad2*$^{fl/fl}$ healing skin compared with controls (Fig. 4, *C* and *D*; $p < 0.05$, $n = 5$). Similar to that in Ppm1a-null mice, the rate of proliferative keratinocytes at wound edge was equivalent in both *K5-Cre;Smad2*$^{fl/fl}$ and control mice (Fig. 4, *E* and *F*). Moreover, migration of Smad2 deficient keratinocytes was significantly enhanced by 41% compared with control cells at 48 h in an *in vitro* scratch assay (Fig. 4, *G* and *H*; $p < 0.01$), indicating that accelerated re-epithelialization observed in Smad2-deficient mice was associated with enhanced keratinocyte migration.

Simultaneous Deletion of Smad2 and Ppm1a Accelerated Re-epithelialization Rate—To further confirm that whether or not Smad2 is required for Ppm1a-regulated re-epithelialization, we generated Smad2 and Ppm1a double mutant mice. Western blot confirmed that the expression of both Smad2 and Ppm1a was significantly downregulated in primary keratinocytes of *K5-Cre;Smad2*$^{fl/fl}$*;Ppm1a*$^{-/-}$ *mice* (Fig. 5*A*). As expected, the rate of re-epithelialization was dramatically accelerated in *K5-Cre;Smad2*$^{fl/fl}$*;Ppm1a*$^{-/-}$ mice compared with controls (Fig. 5, *B–D*; $p < 0.05$). Furthermore, the rate of scratch closure from double mutant keratinocytes was notably faster by 45% than that from controls at 48 h after wounding (Fig. 5, *E* and *F*; $p < 0.01$). The above data demonstrated that the effect of Ppm1a on promoting re-epithelialization is mediated by Smad2 signaling, at least during cutaneous wound healing.

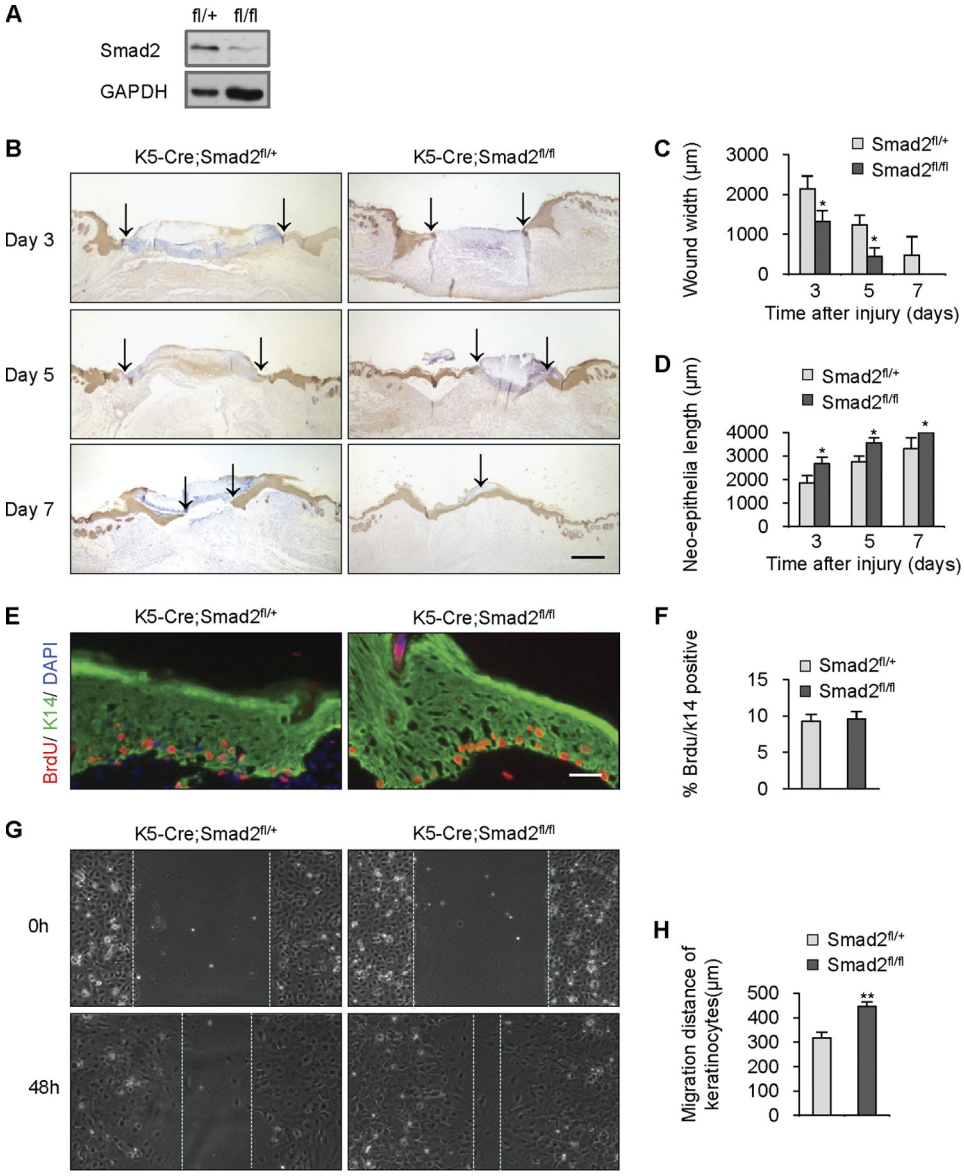

FIGURE 4. **Keratinocyte-specific deletion of Smad2 resulted in accelerated re-epithelialization during wound healing.** *A*, Western blot analysis demonstrated that Smad2 expression was dramatically decreased in the primary keratinocytes from *K5-Cre;Smad2*$^{fl/fl}$ mice. *B*, wound widths were determined by K14 (*brown*) immunostaining in *K5-Cre;Smad2*$^{fl/fl}$ and control wounded skin at days 3, 5, and 7 after injury. *Arrows* indicated the leading edges of wounded epidermis. *C* and *D*, quantification of wound width and neo-epithelia length over 7 days after injury. $n = 5$. *E*, immunofluorescence staining with BrdU (*red*) and K14 (*green*) antibodies was performed at day 3 after injury in *K5-Cre;Smad2*$^{fl/fl}$ and control wound sections. *F*, quantification of the percentage of BrdU positive keratinocytes; $n = 3$. *G*, confluent *K5-Cre;Smad2*$^{fl/fl}$ and control keratinocytes were wounded by scraping. Migration distance was measured at 0, 48 h after cells were scratched. *H*, quantification of migration distance; $n = 3$. Values represent mean ± S.D. *, $p < 0.05$; **, $p < 0.01$. Scale bars: 400 μm (*B*); 50 μm (*E*).

Altered Expression of Integrins and MMPs in Ppm1a Mutant Mice—During the re-epithelialization process, keratinocytes should be able to detach from the underlying basal lamina and migrate through the fibrin and extracellular matrix (ECM) meshwork of the wound. Two classes of molecules, the integrins and matrix metalloproteinases (MMPs), have been shown to facilitate keratinocyte migration during wound healing (34, 35). We examined integrins and MMPs expression in Ppm1a single mutant, Smad2 single mutant or Ppm1a and Smad2 double mutant mice by real-time PCR assay. At day 3 post-injury, the expression levels of integrin β1, integrin α5, integrin αv, MMP13, and MMP2 were apparently down-regulated at *K5-Cre; Ppm1a*$^{fl/fl}$ wound edge compared with that at control wound edge (Fig. 6; $p < 0.01$). Conversely, the expression of the above molecules were up-regulated in Smad2 single deficient mice or Ppm1a and Smad2 double mutant mice compared with corresponding controls (Fig. 6; $p < 0.05$). In addition, similar changes of the above integrins and MMPs were found in complete Ppm1a gene knock-out mice (supplemental Fig. S4). These expression differences of key effectors of keratinocyte movement likely contributed to the delayed wound closure in Ppm1a-deficient mice.

DISCUSSION

There are three novel findings in the present study. First, deletion of Ppm1a is dispensable for embryonic development and adult homeostasis; second, deletion of Ppm1a leads to delayed re-epithelialization during wound healing

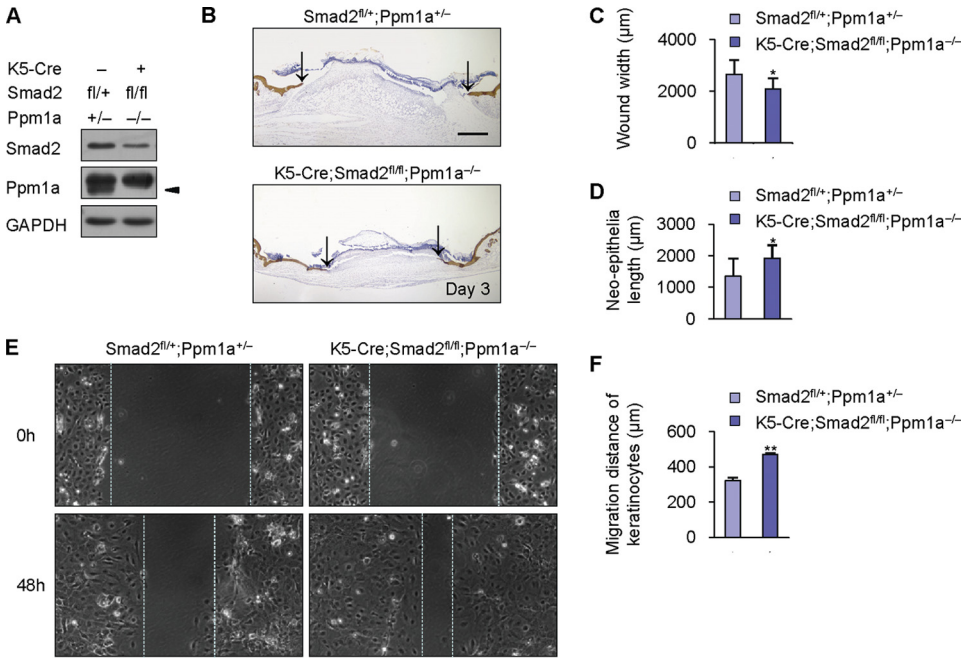

FIGURE 5. **Simultaneous deletion of Smad2 and Ppm1a accelerated re-epithelialization rate.** *A*, Western blot showed that the expression of Smad2 and Ppm1a were significantly reduced in the primary keratinocytes from *K5-Cre;Smad2$^{fl/fl}$;Ppm1a$^{-/-}$* mice. *Arrows* indicated the specific band of Ppm1a. *B*, K14 (*brown*) immunostaining of the sections of wounded skin in *K5-Cre;Smad2$^{fl/fl}$;Ppm1a$^{-/-}$* mice and control mice at day 3 after injury. *Arrows* indicated the leading edges of wounded epidermis. *C* and *D*, quantification of wound width and neo-epithelia length at day 3 after injury. $n = 4$. *E*, confluent *K5-Cre;Smad2$^{fl/fl}$;Ppm1a$^{-/-}$* and control keratinocytes were wounded by scraping. Migration distance was measured at 0, 48 h after cells were scratched. *H*, quantification of migration distance; $n = 3$. Values represent mean ± S.D. *, $p < 0.05$; **, $p < 0.01$. Scale bars: 400 μm (*B*).

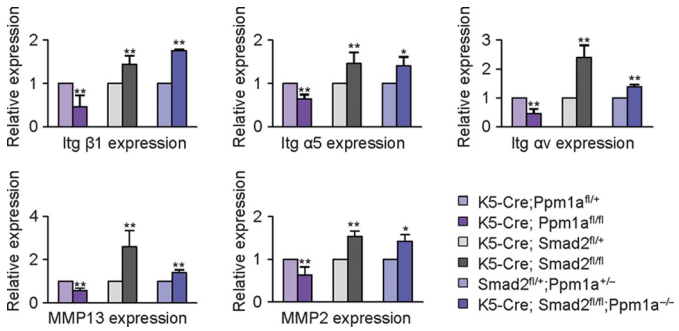

FIGURE 6. **Altered expression of specific integrins and MMPs in Ppm1a single mutant, Smad2 single mutant, or Ppm1a and Smad2 double mutant mice.** Real-time PCR was carried out using RNAs isolated from *K5-Cre;Ppm1a$^{fl/fl}$*, *K5-Cre;Smad2$^{fl/fl}$*, *K5-Cre;Smad2$^{fl/fl}$;Ppm1a$^{-/-}$* and their littermate control wound edge. The expression of integrin β1(Itgβ1), Itg α5, Itg αv, MMP13, and MMP2 was quantified and normalized to GAPDH; $n = 3$. Values represent mean ± S.D. *, $p < 0.05$; **, $p < 0.01$.

via decreased keratinocyte migration; third, Ppm1a can repress overactivation of Smad2 signaling, which is inhibitory for epidermal cell migration in wound healing. Taken together, we identified, for the first time, the pathophysiological role of Ppm1a in re-epithelialization process during wound healing.

We provided the first and critical *in vivo* genetic evidence showing a role of Ppm1a in promoting keratinocyte migration during wound healing. Ppm1a has been shown to regulate cell proliferation and cell differentiation *in vitro* (19, 21). A recent study has revealed that PPM1A is involved in human cytrophoblast cell migration (36). Although PPM1A decreases the growth-inhibitory effect of TGF-β via dephosphorylating Smad2/3 in HaCaT cell (19), an immortalized human keratinocyte cell line, the role of PPM1A in keratinocyte migration is largely unknown. In this study, skin development and homeostasis were normal in both complete and conditional keratinocyte specific Ppm1a mutant mice, which suggested functional redundancy of other members of Ppm1 family in skin formation. However, under conditions of the cutaneous stress response, the function of Ppm1a during re-epithelialization process is indispensable. Deletion of Ppm1a led to delayed re-epithelialization due to the retarded keratinocyte migration, but not due to altered keratinocyte proliferation (Figs. 1 and 2). More importantly, we found that the phenotypes were identical between complete and epiderm-specific Ppm1a mutant mice, suggesting that Ppm1a in keratinocyte, but not in other cell types, is required for normal re-epithelialization process. Consistent with the notion, Ppm1a is expressed at high levels in epidermis, but at very low levels in dermal fibroblasts, vessels, and microvasculature (37).

Growing evidence has shown that Ppm1a could dephosphorylate its distinct targets to control particular cellular activities (19, 21). Here, we first exemplified that Ppm1a could suppress Smad2 signaling, thereby promoting keratinocyte migration and re-epithelialization during wound healing. Deletion of Ppm1a elevated the expression level of p-Smad2 at wound edge post-wounding (Fig. 3, *A* and *B*) and in primary isolated keratinocytes (Fig. 3*C*). Consistently, a previous study has indicated that overexpression of Smad2 is inhibitory for re-epithelialization (12). Delayed wound healing because of retarded keratinocyte migration has been found in the Smad2 transgenic mice (12), which is quite similar to that observed in Ppm1a mutant mice. To support this notion, in this study, we showed that keratinocyte-specific Smad2 deletion led to accelerated re-epithelialization caused by the enhanced keratinocyte migration. Similar to the phenotypes found in Smad2 single mutant mice,

Smad2 and Ppm1a double mutant mice exhibited accelerated re-epithelialization rate, strongly suggesting that Smad2 is required for Ppm1a-regulated re-epithelialization. Moreover, the inverse expression patterns of specific integrins and MMPs in Ppm1a-null and Smad2-null mice or Ppm1a and Smad2 double mutant mice suggested that Ppm1a might modulate expression of the above effectors possibly through its Smad2-antagonizing activity. During wound healing, Ppm1a expression at wound edge was down-regulated (Fig. 1*A*), and accordingly, p-Smad2/3 expression was gradually increased post-wounding (Fig. 3*A*). This raises an interesting question of what mechanism by which Ppm1a was regulated, thereby influencing Smad2 signaling. Further study involved in regulation of Ppm1a would provide new insights into the role of Ppm1a in fine tuning diverse signals during wound healing process.

Our present study provided new evidence supporting the notion that TGF-β/Smad signaling plays an inhibitory role in re-epithelialization during skin wound healing, at least in the full thickness wound scenario. We found that mice deficient in Ppm1a, which exhibited overactivation of Smad2, displayed significantly decreased re-epithelialization, demonstrating that epidermal TGF-β/Smad signaling repressed re-epithelialization. Smad2 mutant mice showed the opposite phenotypes, further supporting the point of view. Consistently, many previous *in vivo* studies have indicated that TGF-β/Smad signaling suppresses wound re-epithelialization. The re-epithelialization of full thickness wounds is delayed in TGF-β1, BMP6, or Smad2 overexpressing transgenic mice (10, 12–14), and accelerated in mice expressing a dominant-negative type II TGF-β receptor (8) or Smad3-null mice (9). In contrast, the results from the mice with deletion of TGF-β1 or Smad4, and mice overexpressing activin A, suggest a positive role of TGF-β/Smad signaling in re-epithelialization (5–7). These obvious discrepancies might largely due to various effects of TGF-β signaling mediated by different cell types involved in wound healing. Future studies using various cell- and stage-specific genetically modified mice will be crucial to better define the effect of TGF-β/Smad signaling on wound re-epithelialization.

Acknowledgments—We thank Chuxia Deng and Fen Zhou for kindly providing the TC1 ES cells.

REFERENCES

1. Gurtner, G. C., Werner, S., Barrandon, Y., and Longaker, M. T. (2008) *Nature* **453,** 314–321
2. Werner, S., and Grose, R. (2003) *Physiol. Rev.* **83,** 835–870
3. Padua, D., and Massagué, J. (2009) *Cell Res.* **19,** 89–102
4. Schmierer, B., and Hill, C. S. (2007) *Nat. Rev. Mol. Cell Biol.* **8,** 970–982
5. Crowe, M. J., Doetschman, T., and Greenhalgh, D. G. (2000) *J. Invest. Dermatol* **115,** 3–11
6. Munz, B., Smola, H., Engelhardt, F., Bleuel, K., Brauchle, M., Lein, I., Evans, L. W., Huylebroeck, D., Balling, R., and Werner, S. (1999) *EMBO J.* **18,** 5205–5215
7. Owens, P., Engelking, E., Han, G., Haeger, S. M., and Wang, X. J. (2010) *Am. J. Pathol.* **176,** 122–133
8. Amendt, C., Mann, A., Schirmacher, P., and Blessing, M. (2002) *J. Cell Sci.* **115,** 2189–2198
9. Ashcroft, G. S., Yang, X., Glick, A. B., Weinstein, M., Letterio, J. L., Mizel, D. E., Anzano, M., Greenwell-Wild, T., Wahl, S. M., Deng, C., and Roberts, A. B. (1999) *Nat. Cell Biol.* **1,** 260–266
10. Chan, T., Ghahary, A., Demare, J., Yang, L., Iwashina, T., Scott, P. G., and Tredget, E. E. (2002) *Wound Repair Regen.* **10,** 177–187
11. Garlick, J. A., and Taichman, L. B. (1994) *J. Invest. Dermatol.* **103,** 554–559
12. Hosokawa, R., Urata, M. M., Ito, Y., Bringas, P., Jr., and Chai, Y. (2005) *J. Invest. Dermatol.* **125,** 1302–1309
13. Kaiser, S., Schirmacher, P., Philipp, A., Protschka, M., Moll, I., Nicol, K., and Blessing, M. (1998) *J. Invest. Dermatol.* **111,** 1145–1152
14. Tredget, E. B., Demare, J., Chandran, G., Tredget, E. E., Yang, L., and Ghahary, A. (2005) *Wound Repair Regen.* **13,** 61–67
15. Wang, X. J., Han, G., Owens, P., Siddiqui, Y., and Li, A. G. (2006) *J. Investig Dermatol. Symp. Proc.* **11,** 112–117
16. Meng, F., Cheng, X., Yang, L., Hou, N., Yang, X., and Meng, A. (2008) *J. Cell Sci.* **121,** 2904–2912
17. Reynolds, L. E., Conti, F. J., Lucas, M., Grose, R., Robinson, S., Stone, M., Saunders, G., Dickson, C., Hynes, R. O., Lacy-Hulbert, A., and Hodivala-Dilke, K. (2005) *Nat. Med.* **11,** 167–174
18. Reynolds, L. E., Conti, F. J., Silva, R., Robinson, S. D., Iyer, V., Rudling, R., Cross, B., Nye, E., Hart, I. R., Dipersio, C. M., and Hodivala-Dilke, K. M. (2008) *J. Clin. Invest.* **118,** 965–974
19. Lin, X., Duan, X., Liang, Y. Y., Su, Y., Wrighton, K. H., Long, J., Hu, M., Davis, C. M., Wang, J., Brunicardi, F. C., Shi, Y., Chen, Y. G., Meng, A., and Feng, X. H. (2006) *Cell* **125,** 915–928
20. Takekawa, M., Maeda, T., and Saito, H. (1998) *EMBO J.* **17,** 4744–4752
21. Yoshizaki, T., Maegawa, H., Egawa, K., Ugi, S., Nishio, Y., Imamura, T., Kobayashi, T., Tamura, S., Olefsky, J. M., and Kashiwagi, A. (2004) *J. Biol. Chem.* **279,** 22715–22726
22. Cheng, A., Ross, K. E., Kaldis, P., and Solomon, M. J. (1999) *Genes Dev.* **13,** 2946–2957
23. Strovel, E. T., Wu, D., and Sussman, D. J. (2000) *J. Biol. Chem.* **275,** 2399–2403
24. Duan, X., Liang, Y. Y., Feng, X. H., and Lin, X. (2006) *J. Biol. Chem.* **281,** 36526–36532
25. Schilling, S. H., Datto, M. B., and Wang, X. F. (2006) *Cell* **125,** 838–840
26. Kokabu, S., Nojima, J., Kanomata, K., Ohte, S., Yoda, T., Fukuda, T., and Katagiri, T. *J. Bone Miner Res.* **25,** 653–660
27. Weinstein, M., Yang, X., Li, C., Xu, X., Gotay, J., and Deng, C. X. (1998) *Proc. Natl. Acad. Sci. U.S.A.* **95,** 9378–9383
28. Lakso, M., Pichel, J. G., Gorman, J. R., Sauer, B., Okamoto, Y., Lee, E., Alt, F. W., and Westphal, H. (1996) *Proc. Natl. Acad. Sci. U.S.A.* **93,** 5860–5865
29. Teng, Y., Sun, A. N., Pan, X. C., Yang, G., Yang, L. L., Wang, M. R., and Yang, X. (2006) *Cancer Res.* **66,** 6972–6981
30. Yang, L., Mao, C., Teng, Y., Li, W., Zhang, J., Cheng, X., Li, X., Han, X., Xia, Z., Deng, H., and Yang, X. (2005) *Cancer Res.* **65,** 8671–8678
31. Squarize, C. H., Castilho, R. M., Bugge, T. H., and Gutkind, J. S. (2010) *PLoS One* **5,** e10643
32. Zhou, J., Cheng, X., Sun, Y., Huang, P., Huang, C., and Yang, X. (2002) *Sci. China C Life Sci.* **45,** 129–137
33. Hoot, K. E., Lighthall, J., Han, G., Lu, S. L., Li, A., Ju, W., Kulesz-Martin, M., Bottinger, E., and Wang, X. J. (2008) *J. Clin. Invest.* **118,** 2722–2732
34. Margadant, C., Charafeddine, R. A., and Sonnenberg, A. (2010) *FASEB J.* **24,** 4133–4152
35. Page-McCaw, A., Ewald, A. J., and Werb, Z. (2007) *Nat. Rev. Mol. Cell Biol.* **8,** 221–233
36. Zhang, B., Zhou, Z., Lin, H., Lv, X., Fu, J., Lin, P., Zhu, C., and Wang, H. (2009) *Histochem. Cell Biol.* **132,** 169–179
37. Lifschitz-Mercer, B., Sheinin, Y., Ben-Meir, D., Bramante-Schreiber, L., Leider-Trejo, L., Karby, S., Smorodinsky, N. I., and Lavi, S. (2001) *Histochem. Cell Biol.* **116,** 31–39